Electron Microscopy of Coronavirus-Like Particles Characteristic of Turkey Bluecomb Disease
Author(s): A. E. Ritchie, D. R. Deshmukh, C. T. Larsen and B. S. Pomeroy
Source: *Avian Diseases*, Vol. 17, No. 3 (Jul. - Sep., 1973), pp. 546-558
Published by: American Association of Avian Pathologists
Stable URL: http://www.jstor.org/stable/1589153
Accessed: 29-11-2015 15:09 UTC

REFERENCES
Linked references are available on JSTOR for this article:
http://www.jstor.org/stable/1589153?seq=1&cid=pdf-reference#references_tab_contents

You may need to log in to JSTOR to access the linked references.

Your use of the JSTOR archive indicates your acceptance of the Terms & Conditions of Use, available at http://www.jstor.org/page/info/about/policies/terms.jsp

JSTOR is a not-for-profit service that helps scholars, researchers, and students discover, use, and build upon a wide range of content in a trusted digital archive. We use information technology and tools to increase productivity and facilitate new forms of scholarship. For more information about JSTOR, please contact support@jstor.org.

American Association of Avian Pathologists and Allen Press are collaborating with JSTOR to digitize, preserve and extend access to *Avian Diseases*.

http://www.jstor.org

This content downloaded from 160.36.178.25 on Sun, 29 Nov 2015 15:09:47 UTC
All use subject to JSTOR Terms and Conditions

Electron Microscopy of Coronavirus-like Particles Characteristic of Turkey Bluecomb Disease[A]

A. E. Ritchie, D. R. Deshmukh, C. T. Larsen, and B. S. Pomeroy

Received 9 February 1973

SUMMARY

Particles morphologically similar to coronaviruses were found in bluecomb-infected turkey ceca, the bursa of Fabricius, and embryo intestines, but not in the same tissues of uninfected controls. The particles had diameters ranging from *ca.* 50 to >150 nm and bore variable numbers of pear- or club-shaped projections. None had a morphologically distinct organized internal component. The concentration of corona-virus-like particles (CVLP) was highest in embryo intestine and lowest in poult ceca and paralleled infectivity. The CVLP reacted specifically with antibodies in hyperimmune anti-bluecomb turkey serum but not with components of normal turkey serum or antibodies against 4 different coronaviruses. These CVLP appear to be characteristically associated with bluecomb disease and probably represent the infectious agent. Small oblate ellipsoidal particles, 20 × 45 nm, consisting of 2 curved portions fused at their ends were also uniquely associated with bluecomb infection and may represent viral precursors.

INTRODUCTION

The viral etiology of the bluecomb disease (transmissible enteritis) has been suspected for many years (13). Filterability of the infectious agent was demonstrated (18) as early as 1957. More recently, the agent was found to pass through 100-nm membrane filters and to be sensitive to lipid solvents, acid pH, and heating at 50 C for 1 hour (7,8). Its buoyant density in buffered sucrose solution has been estimated at 1.24 g/cm^3.

[A]Presented in part at the 53rd Annual Meeting of the Conference of Research Workers in Animal Disease, November 27-28, 1972, Chicago, Illinois.

From the National Animal Disease Laboratory, North Central Region, Agricultural Research Service, U.S. Department of Agriculture, Ames, Iowa 50010; and Department of Veterinary Microbiology and Public Health, College of Veterinary Medicine, University of Minnesota, St. Paul, Minnesota 55101.

This content downloaded from 160.36.178.25 on Sun, 29 Nov 2015 15:09:47 UTC
All use subject to JSTOR Terms and Conditions

Virus-like particles maturing from intracytoplasmic membranes have been detected (2) in thin sections of tissues from bluecomb-infected turkey poults and embryos. Adams *et al.* described these particles as "enveloped" with diameters ranging from 50 to 120 nm. In a subsequent report (3), they described a population of highly pleomorphic particles observed in phosphotungstate (PTA) negatively stained preparations of bluecomb-infected turkey embryo intestines. These pleomorphic particles had a size range of 60 to 250 nm and bore "tubular surface projections" suggesting a morphological similarity to influenza virus. No hemagglutinating activity could be demonstrated for these particles. In support of their conclusion that the "myxovirus"-like particles were bluecomb virions, they described (3) short rigid rods believed to represent an "internal component" usually seen as aggregates of helically structured fibers measuring about 7 nm in diameter.

Our initial electron-microscope studies of bluecomb-infected adult turkey ceca failed to identify any virus-like particles characteristically associated with the disease (16). We attributed the failure to the ubiquity of a variety of bacteria, phages, and bacterial cell fragments. This suggested that we examine infected tissues from turkey poults and embryos since their microbial flora would likely be less complex.

The present report describes our observations of CVLP regularly found in bluecomb-infected poult ceca and bursae, and embryo intestines. These particles react specifically with bluecomb antibodies and thus appear to be characteristically associated with bluecomb infection.

MATERIALS AND METHODS

Virus. Infective filtrates from turkeys considered to have had bluecomb (Minnesota strain) were prepared as previously described (7). Poults (1–5 days old) were inoculated orally with a 1-ml dose of infective cecal material. Embryos (24 days old) were inoculated in the amniotic cavity with a 0.2-ml dose of infective bursal material. The bursae of Fabricius and ceca of infected birds were sampled at 72 or 96 hours postinfection. Virus titer was 3 $\log_{10}$ PID (poult infectivity dose) in the bursa of Fabricius and 2 $\log_{10}$ PID in the cecum. Infected embryos were harvested after 3 days of incubation at 37 C; intestinal filtrates had a virus titer of at least 4 $\log_{10}$ PID (first passage) and 2 $\log_{10}$ PID (22nd passage).

Centrifugation. Before electron microscopy, most tissue homogenates and filtrates were centrifuged at 16,000 $\times$ g for 35 minutes

This content downloaded from 160.36.178.25 on Sun, 29 Nov 2015 15:09:47 UTC
All use subject to JSTOR Terms and Conditions

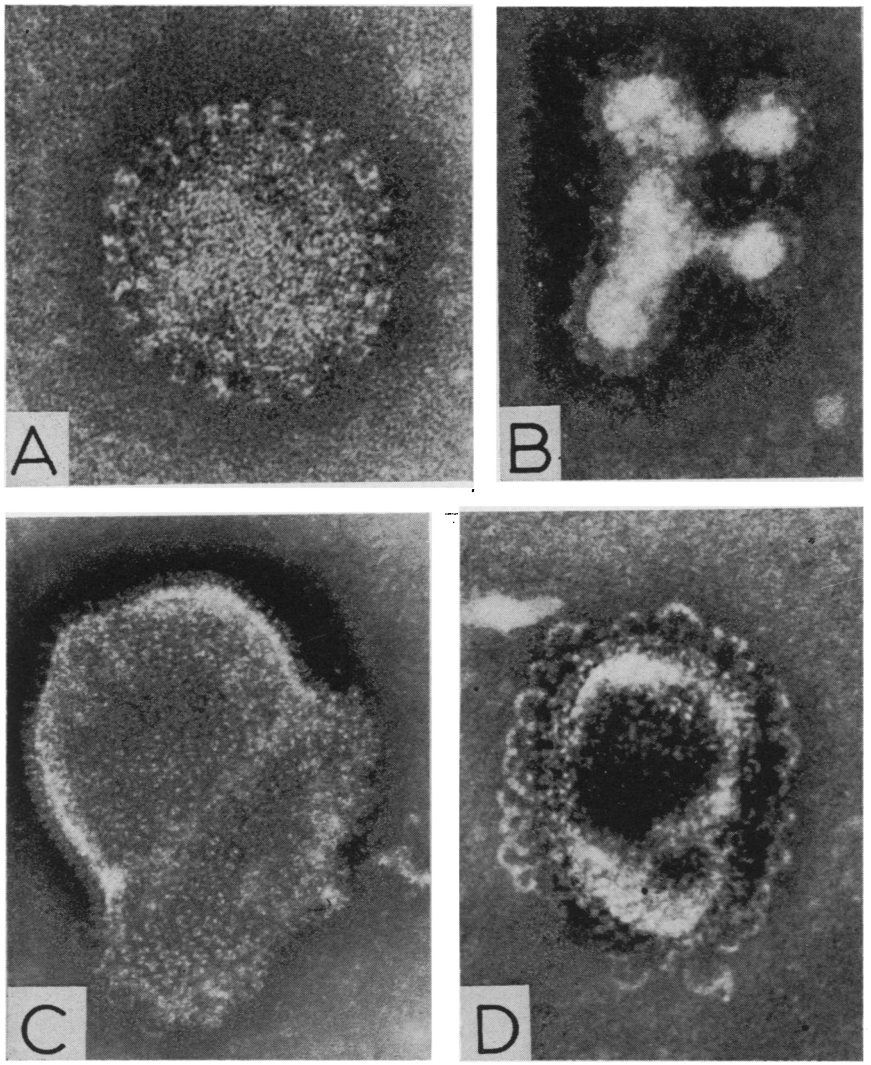

Fig. 1. Negatively stained particles commonly found in both uninfected and bluecomb-infected turkey tissues. A) Small typical spherical particle marked by distinctive close-packed surface projections. ×400,000. B) Pleomorphic particle with projections similar to *A* but undergoing subdivision by pinching-off. ×350,000. C) Large collapsed particle with projections similar to *A* but with ruptured membrane at lower right. No internal structure is evident. ×160,000. D) Particle similar to *A* but with surface sloughing by transformation of projections into arc-shaped structures. ×270,000.

This content downloaded from 160.36.178.25 on Sun, 29 Nov 2015 15:09:47 UTC
All use subject to JSTOR Terms and Conditions

to concentrate particulate entities with diameters greater than *ca.* 50 nm. Sedimented particles were resuspended in distilled water with gentle magnetic stirring.

Hyperimmune anti-bluecomb turkey serum. Three 12-week-old turkeys were orally given a 20% cecal suspension prepared from acutely affected poults whose ceca were harvested at *ca.* 4 days postinoculation. Each bird then received 3–5 ml of inoculum orally at 5-day intervals for 25 days. Seven days after the last inoculum, they were bled by cardiac puncture. The pooled serum neutralized at least 3 $\log_{10}$ of cecal infectivity when assayed in day-old turkey poults. It also neutralized at least 2 $\log_{10}$ PID of egg-passaged bluecomb infectivity.

Electron microscopy. Homogenates and filtrates of turkey tissues containing 0.5–1.0% potassium phosphotungstate were applied to carbon-coated collodion-filmed grids with an all-glass nebulizer as described previously (15).

Direct immuno-electron microscopy. Tissue homogenates or infective filtrates were incubated at 4 C for 18 hours with hyperimmune anti-bluecomb turkey serum. Antigen-antibody complexes and unreacted particles were co-sedimented by centrifugation at 16,000 $\times$ *g* for 35 minutes. The sediment was suspended in distilled water with gentle magnetic stirring before negative staining. To test for possible antigenic relationships, the infectious preparations were similarly processed with antisera against 4 coronaviruses: avian infectious bronchitis (4), hemagglutinating encephalomyelitis of swine (9), a cytopathogenic agent associated with transmissible gastroenteritis of swine (11,14), and an agent isolated from field outbreaks of neonatal calf diarrhea (17).

Controls. Bursal and cecal homogenates and filtrates were prepared from bluecomb-free poults and examined in PTA. Uninfected embryo intestine was similarly prepared and examined. Normal turkey serum with no measurable bluecomb-neutralizing titer and antisera to the 4 non-bluecomb coronaviruses were incubated with preparations from uninfected tissue to determine whether any specific immune reactions could be detected by electron microscopy.

RESULTS

Controls. Homogenates and filtrates from uninfected turkey tissues contained numerous particulate entities ranging in size from <10 to >200 nm. Most had a grossly irregular morphology, as though they were sheared fragments of cellular structures.

This content downloaded from 160.36.178.25 on Sun, 29 Nov 2015 15:09:47 UTC
All use subject to JSTOR Terms and Conditions

Many had regular contours and were generally round or oblong. Two ubiquitous types of cell derivatives, examined in detail, are illustrated in Figs. 1 and 2.

The most common particulates were typically smooth-contoured and covered with uniform close-packed projections (Fig. 1A). The projections were *ca.* 10 nm long, with center-to-center spacings of 10 nm, giving the appearance of tubular structures. Particles bearing these projections ranged from <50 to >200 nm. Frequently they were pleomorphic and underwent subdivision by budding (Fig. 1B). When collapsed or fragmented, none showed any evidence of an organized internal component (Fig. 1C). Some of them sloughed their surface components by a characteristic micellar transformation (Fig. 1D). None of these particles reacted with antibodies in hyperimmune anti-bluecomb turkey serum, normal turkey serum, or antisera to the 4 non-bluecomb coronaviruses.

The other commonly encountered particulate entities consisted of aggregates of thin rodlets (Fig. 2). These rodlets had an average diameter of *ca.* 4 nm, a maximum individual length of *ca.* 140 nm, and a 3.5-nm helical periodicity (Fig. 2). They did not react with

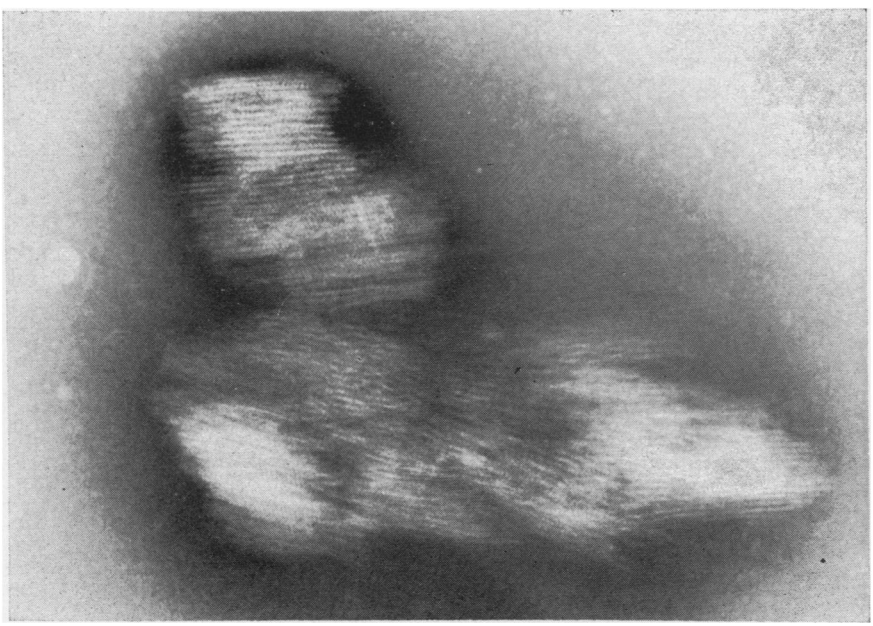

Fig. 2. Negatively stained aggregates of thin (4-nm) helical rods present in both uninfected and bluecomb-infected turkey tissues. ×160,000.

This content downloaded from 160.36.178.25 on Sun, 29 Nov 2015 15:09:47 UTC
All use subject to JSTOR Terms and Conditions

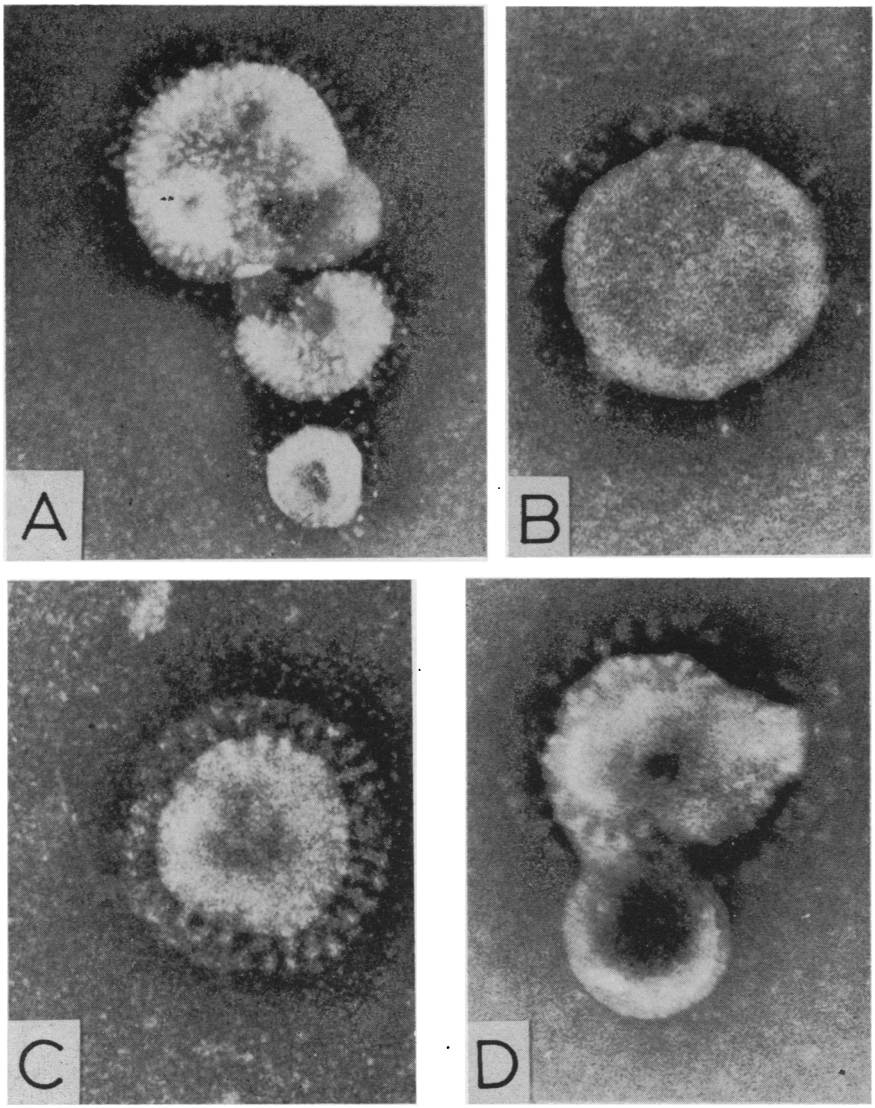

Fig. 3. Negatively stained coronavirus-like particles characteristically associated with bluecomb-infected turkey tissues. A) Three particles with identifying 15-to-20-nm pear- or club-shaped surface projections illustrating representative particle size variation. ×170,000. B) Frequently encountered type illustrating sparsity of its surface projections. ×300,000. C) Infrequently encountered type illustrating maximum packing of its surface projections. ×300,000. D) Commonly encountered type with distended membrane (lower right). Note absence of surface projections on the blebbed portion. ×300,000.

This content downloaded from 160.36.178.25 on Sun, 29 Nov 2015 15:09:47 UTC
All use subject to JSTOR Terms and Conditions

antibodies in the hyperimmune anti-bluecomb turkey serum, normal turkey serum, or antisera to the 4 non-bluecomb coronaviruses.

Bluecomb-infected sources. As expected, the predominant particulate entities in all infective homogenates or filtrates were indistinguishable from cellular derivatives noted in control preparations. In addition, all infective sources contained a population of particles not found in controls whose morphology resembled mem-

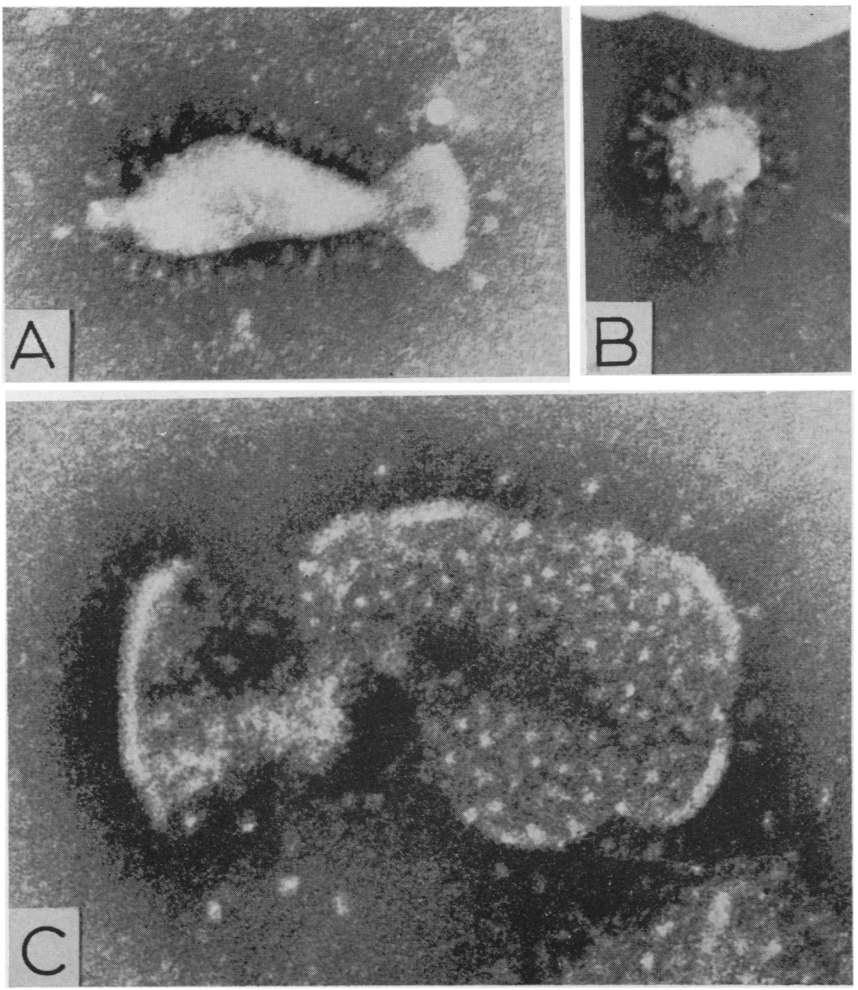

Fig. 4. Negatively stained coronavirus-like particles characteristically associated with bluecomb-infected turkey tissues. A) Pleomorphic particle illustrating initial stages of subdivision by "pinching off" to produce particles of various size. ×280,000. B) Small particle (<70 nm) illustrating close packing of typical surface projections. ×280,000. C) Disrupted particle illustrating absence of an organized internal component. ×375,000.

This content downloaded from 160.36.178.25 on Sun, 29 Nov 2015 15:09:47 UTC
All use subject to JSTOR Terms and Conditions

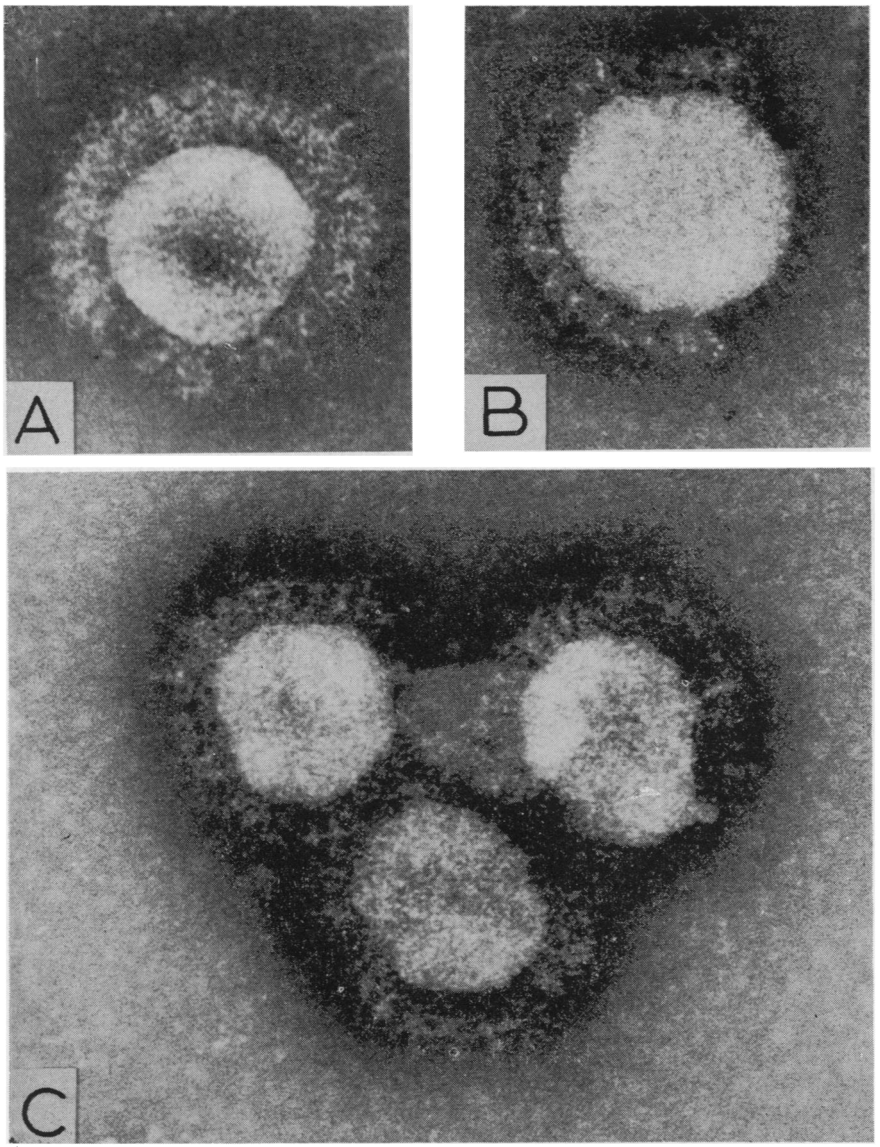

Fig. 5. Negatively stained antigen-antibody complexes of coronavirus-like particles after 18 hours of incubation in an excess of hyperimmune anti-bluecomb turkey serum. A) Single particle with near-uniform coating of antibody molecules obscuring the image of its surface projections. ×350,000. B) Single particle illustrating localization of antigen-antibody reaction over only the left two-thirds of its surface. ×300,000. C) Aggregate of 3 particles agglutinated by antibody molecules. Agglutination was concentration dependent and most readily observed with embryo intestinal preparations. ×300,000.

This content downloaded from 160.36.178.25 on Sun, 29 Nov 2015 15:09:47 UTC
All use subject to JSTOR Terms and Conditions

bers of the coronavirus group. They ranged in size from *ca.* 50 to >150 nm and tended to aggregate (Fig. 3A). Most had diameters of 90–120 nm. Their surfaces bore pear- or club-shaped projections (15–20 nm) in various numbers. Some had fewer than 10 projections (Fig. 3B) or more than 100 (Fig. 3C). Some were blebbed, exposing large areas of naked membrane (Fig. 3D). The smallest recognizable particles of this type appeared to arise by "pinching-off" (Figs. 4A and B). Fragments of membrane that bore pear-shaped projections were found occasionally. Neither intact nor disrupted particles revealed an organized internal component, which would have suggested a discrete subviral infective unit (Fig. 4C).

After incubation with hyperimmune anti-bluecomb turkey serum these particles were coated with antibody, thereby obscuring their typical appearance (Fig. 5A) and increasing their diameter by *ca.* 20 nm. On particles with naked areas, the antigen-antibody reaction was localized at sites of the surface projections

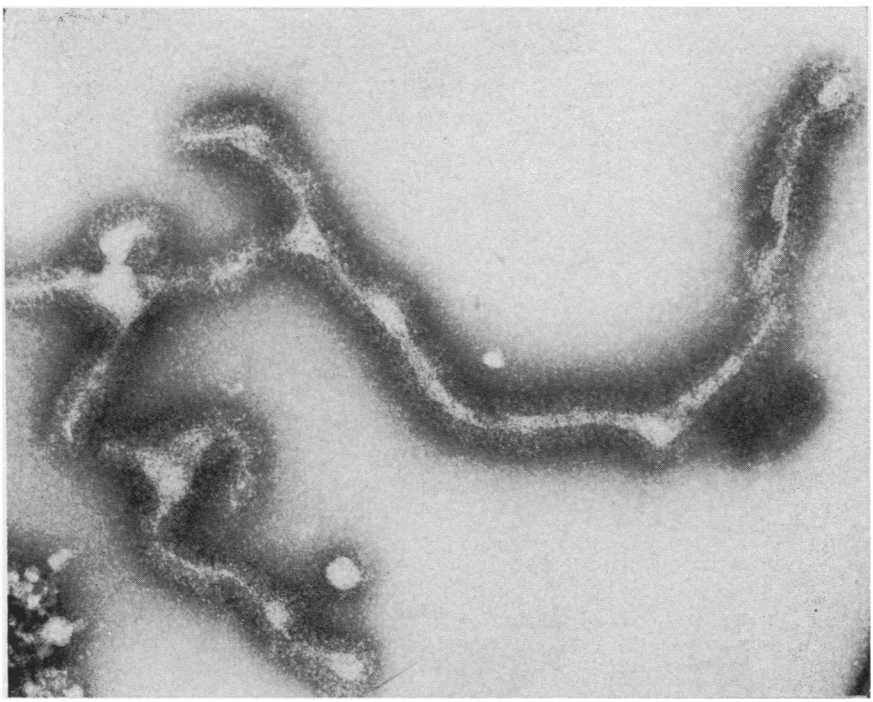

Fig. 6. Negatively stained bluecomb-infected turkey tissue membrane fragment uniformly coated with anti-bluecomb antibodies indicating the presence of virus-specific antigen. ×140,000.

This content downloaded from 160.36.178.25 on Sun, 29 Nov 2015 15:09:47 UTC
All use subject to JSTOR Terms and Conditions

(Fig. 5B). When the particle concentration was sufficiently high, e.g., in infected embryo intestine, aggregates of these antigen-antibody complexes were formed (Fig. 5C). Small particles and fragments of membrane were also coated with antibodies from the hyperimmune serum, confirming the presence of bluecomb-specific antigen (Fig. 6). No other particulate entities in any of the infective sources showed evidence of reaction with antibodies from the hyperimmune serum. Neither particles nor membranous structures bearing the typical coronavirus surface projections were affected by incubation with normal turkey serum or antisera against the known coronaviruses.

Incidence of CVLP in the various preparations (either free or as antigen-antibody complexes) depended upon their source. As a crude quantitative reference point we estimated their frequency relative to the cellular derivatives illustrated in Fig. 1. For the 3 sources, this ratio of coronavirus-like particles to normal cell particles was: 1:20 for embryo intestine, 1:100 for poult bursa,

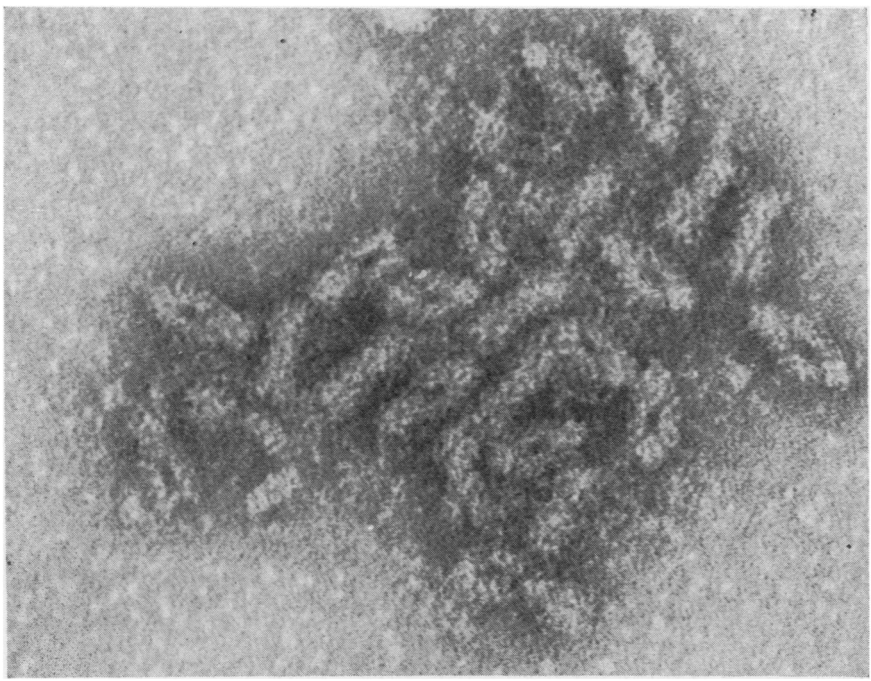

Fig. 7. Negatively stained cluster of small oblate structures (20 × 45 nm) with hollow centers from bluecomb-infected turkey tissue. ×380,000.

This content downloaded from 160.36.178.25 on Sun, 29 Nov 2015 15:09:47 UTC
All use subject to JSTOR Terms and Conditions

and 1:500 to 1:1000 for poult cecum. The 22nd egg passage contained fewer characteristic particles than the first passage.

In one infective cecal filtrate, we observed small oblate ellipsoidal particles, 20×45 nm, formed by 2 apposed 8-nm-diameter curved segments fused at their ends (Fig. 7).

DISCUSSION

Of the varied types of particulate entities >50 nm that were encountered, only those with coronavirus morphology were characteristically associated with tissues infected with bluecomb. The frequency of their detection was correlated positively with the infectivity titer of their source. Antibodies in hyperimmune anti-bluecomb turkey serum reacted specifically with these CVLP. From these observations we conclude that they represent characteristic particles of bluecomb disease and should be classified with the coronaviruses.

Since bluecomb antibodies reacted only with those portions of the CVLP bearing typical projections, it is possible that the particle's covering membrane was not strongly antigenic in the turkey.

It was not possible to distinguish infectious from uninfectious particles by morphology. Since the bluecomb infectivity titer of all sources was relatively low, i.e., <5 $\log_{10}$ PID, it seems likely that most of these characteristic particles were uninfectious.

Membranous structures bearing bluecomb-specific antigen may represent a form of cell-associated virus.

The conclusion that bluecomb virus be considered a coronavirus is consistent with its other physical attributes: a buoyant density of *ca.* 1.24 and sensitivity to lipid solvents, acid pH, and heating at 50 C for 1 hour. Its particle size range estimated in our study, *ca.* 50 to >150 nm, is somewhat wider than that reported by Adams *et al.* (2) for particles observed in thin sections of bluecomb-infected turkey poult and embryo cells. The process of bluecomb virus maturation at intracellular membranes proposed by Adams *et al.* (2) is typical of that described for other coronaviruses, e.g., mouse hepatitis virus (6), infectious bronchitis virus (5,10), and the Linder strain of human coronavirus (12).

The small ellipsoidal particles found in a cecal filtrate were similar to viral precursor materials observed intracytoplasmically in cells infected with a human coronavirus (12).

The smooth-contoured cellular particles bearing close-packed surface projections found in all our preparations were indistinguishable from the "myxovirus"-like particles described by

This content downloaded from 160.36.178.25 on Sun, 29 Nov 2015 15:09:47 UTC
All use subject to JSTOR Terms and Conditions

Adams *et al.* (3) and assumed by them to represent bluecomb virions. Those workers did not report any observations made on uninfected control preparations. Since these types of particles were observed in both uninfected and infected tissues in our studies and did not react with bluecomb antibodies, we must conclude that they do not represent characteristic particles etiologically associated with bluecomb.

A similar conclusion must also be reached with regard to the aggregates of thin rodlets found in all our preparations and reported by Adams *et al.* (3) as representing the bluecomb virus "internal component."

The bluecomb characteristic particles did not react with components of normal turkey serum or antibodies against 4 different coronaviruses. This suggests that direct immuno-electron microscopy may serve as a rapid and reliable method for identifying bluecomb virus in other infected tissues.

Recognition that bluecomb characteristic particles have properties similar to other coronaviruses should facilitate their purification for chemical analysis and propagation in cell cultures. Since the ratio of bluecomb characteristic particles to normal cellular derivatives was only about 1:20 in infected embryo intestine, this tissue should serve as a useful source of antigen for the development of additional serological tests.

REFERENCES

1. Adams, N. R., and M. S. Hofstad. Isolation of the agent of transmissible enteritis of turkeys in avian embryos. Avian Dis. 15:426-433. 1971.

2. Adams, N. R., R. A. Ball, C. L. Annis, and M. S. Hofstad. Ultrastructural changes in the intestines of turkey poults and embryos affected with transmissible enteritis. J. Comp. Pathol. 82:187-192. 1972.

3. Adams, N. R., M. S. Hofstad, and P. M. Gough. Physical and morphological characterization of transmissible enteritis virus of turkeys. Avian Dis. 16:817-827. 1972.

4. Almeida, J. D., D. M. Berry, C. H. Cunningham, D. Hamre, M. S. Hofstad, L. Malluci, K. McIntosch, and D. A. J. Tyrrell. Corona-viruses. Nature 220:650. 1968.

5. Becker, W. B., K. McIntosch, J. H. Dees, and R. M. Chanock. Morphogenesis of avian infectious bronchitis virus and a related human virus (strain 229E). J. Virol. 1:1019-1027. 1967.

6. David-Ferreira, J. F., and R. A. Manaker. An electron microscope study of the development of a mouse hepatitis virus in tissue culture cells. J. Cell Biol. 24:57-78. 1965.

7. Deshmukh, D. R., C. T. Larsen, S. K. Dutta, and B. S. Pomeroy. Characterization of pathogenic filtrate and viruses isolated from turkeys with bluecomb. Am. J. Vet. Res. 30:1019-1025. 1969.

8. Hofstad, M. S., N. R. Adams, and M. L. Frey. Studies on a filterable agent associated with infectious enteritis (bluecomb) of turkeys. Avian Dis. 13:386-393. 1969.

This content downloaded from 160.36.178.25 on Sun, 29 Nov 2015 15:09:47 UTC
All use subject to JSTOR Terms and Conditions

9. Mengeling, W. L., A. D. Boothe, and A. E. Ritchie. Characteristics of a coronavirus (strain 67N) of pigs. Am. J. Vet. Res. 33:297-308. 1972.
10. Nazerian, K., and C. H. Cunningham. Morphogenesis of avian infectious bronchitis virus in chicken embryo fibroblasts. J. Gen. Virol. 3:469-470. 1968.
11. Okaniwa, A., K. Harada, and D. K. Park. Structure of swine transmissible gastroenteritis virus examined by negative staining. Natl. Inst. Anim. Health Quart. 8:175-181. 1968.
12. Oshiro, L. S., J. H. Schieble, and E. H. Lennette. Electron microscopic studies of coronavirus. J. Gen. Virol. 12:161-168. 1971.
13. Pomeroy, B. S., and J. M. Sieburth. Bluecomb disease of turkeys. Proc. Am. Vet. Med. Assoc. Mtg. 321-327. 1953.
14. Ritchie, A. E., and J. O. Norman. Characterization of two replicating agents from stock cultures of transmissible gastroenteritis (TGE) of pigs. Bact. Proc. 68:161. 1968.
15. Ritchie, A. E., and A. L. Fernelius. Characterization of bovine viral diarrhea viruses. V. Morphology of characteristic particles studied by electron microscopy. Arch. ges. Virusforsch. 28:369-389. 1969.
16. Ritchie, A. E. Bacteriophages associated with turkey caecums in bluecomb-infected and healthy birds. Proc. 27th Ann. Mtg. Electron Microscopy Society of America. 226-227. 1969.
17. Stair, E. L., M. B. Rhodes, R. G. White, and C. A. Mebus. Neonatal calf diarrhea: Purification and electron microscopy of a coronavirus-like agent. Am. J. Vet. Res. 33:1147-1156. 1972.
18. Tumlin, J. T., B. S. Pomeroy, and R. K. Lindorfer. Bluecomb disease of turkeys. IV. Demonstration of a filterable agent. J. Am. Vet. Med. Assoc. 130:360-365. 1957.

ACKNOWLEDGMENTS

This study was supported in part by grants from the U.S. Department of Agriculture, North Central Region, and the Minnesota Turkey Growers Association.

We thank Mrs. Connie Bissonnette and Mr. William H. Knaack for skillful help in the laboratory.

We greatly appreciate the cooperation of Drs. M. F. Coria, W. L. Mengeling, J. O. Norman, and C. A. Mebus in providing the antisera against other coronaviruses for cross-reaction tests with the bluecomb agent.

This content downloaded from 160.36.178.25 on Sun, 29 Nov 2015 15:09:47 UTC
All use subject to JSTOR Terms and Conditions